

QUASI-3D ANALYTIC MODEL FOR FREE VIBRATION  
ANALYSIS OF SIMPLY SUPPORTED FUNCTIONALLY GRADED  
PLATES (SS-FGP)

SALAH REFRAFI<sup>1</sup>, ABDELAZIZ BOUTRID<sup>1</sup>,  
ABDELHAKIM BOUHADRA<sup>1,2\*</sup>, ABDERRAHMANE MENASRIA<sup>1,2</sup>,  
BELGACEM MAMEN<sup>1,2</sup>

<sup>1</sup>*University of Abbes Lghrour Khenchela,  
Faculty of Sciences & Technology, Civil Engineering Department, Algeria*  
<sup>2</sup>*Materials and Hydrology Laboratory, University of Sidi Bel Abbes,  
Faculty of Technology, Civil Engineering Department, Algeria*

[Received: 23 November 2022. Accepted: 9 March 2023]

doi: <https://doi.org/10.55787/jtams.24.54.1.089>

**ABSTRACT:** This paper uses a quasi-3D shear deformation theory accounting for integral terms and including the stretching effect to study the free vibration of FG plates with simply supported edges. A new function shape is used to show the variation of tangential stresses through the  $z$ -direction of the plate. Poisson's ratio is supposed to be constant, but Young's modulus and densities are assumed to be graded in the thickness direction according to the power law function. The present plate theory satisfies the zero tension on the upper and lower surfaces of the FG plate without using shear correction factors. The equations of motion are obtained via Hamilton's principle and solved using Navier's solution type. The present natural frequencies correspond with the ones in many publications; the outcomes of geometrical ratio, side to thickness ratio, and the material index on the natural frequencies of SS-FGP are investigated.

**KEY WORDS:** SS-FGP; quasi-3D model; stretching effect; free vibration; Hamilton's rule; Navier's solution.

## 1 INTRODUCTION

Functionally graded materials (FGMs) are advanced composite materials that have a continuous variation of material properties from one surface to another, thus eliminating the stress concentration found in laminated composites. The concept of FGMs was first proposed in 1984 by a group of material scientists in Japan, Koizumi [1]. FGMs offer great promise in applications where the operating conditions are severe.

---

\*Corresponding author e-mail: [abdelhakim.bouhadra@univ-khenchela.dz](mailto:abdelhakim.bouhadra@univ-khenchela.dz)

For example, heat exchanger tubes, electrically insulating metal/ceramic joints, and plasma facings for fusion reactors [2–6]. They are also ideal for minimizing thermo-mechanical mismatch in metal-ceramic bonding [7–9].

The wide application of heterogeneous materials with combined characteristics in all fields leads researchers to study their bending, buckling and vibration behavior. The kinematics retained plays a very important role in obtaining the results. Several models have been proposed, beginning with the Love-Kirchhoff model, which is effective only for thin plates because of the neglect of the transverse shear stresses [10, 11], and the Reissner-Mindlin model, which considers the uniform distribution of transverse shear stresses [12, 13] and advanced high order models that consider a parabolic distribution of shear stresses [14–21]. No previous models concede the effect of transverse stretching in their study, which makes their models inaccurate. Many quasi-3D theories exist in the literature as examples to surmount this problem. Zenkour [22] use two-dimensional (2-D) and three-dimensional (3D) analytic solution to study the equilibrium behavior of exponentially functionally graded plate submitted to transversally acting load. The dynamic and the stability behaviors of FG plates taking into account the stretching effect and rotatory inertia, are analyzed by Matsunaga [23]. Neves et al. [24] utilized a new quasi-3D sinusoidal shear deformation theory to analyze the bending and free vibration response of FG plates. Jha et al. [25] presented a free vibration behavior of FG plates based on higher order shear theories accounting for the stretching effect. Batra and Vidoli theory has been used by Sheikholeslami and Saidi [26] to analyze the dynamic behavior without excitation of FG plates based on Winkler-Pasternak elastic foundation. Hebali et al. [27] used refined plate theory (RPT), including the thickness deformation effect, to study the bending and free vibration of FG plates. Alijani and Amabili [28] the nonlinear forced vibrations of FG rectangular plates simply supported movable and immovable boundary conditions edges are investigated by considering the thickness deformation effect. However, most of the previous models are computational costs because of the number of additional unknowns involved. Consequently, a reduced quasi-3D model proposed in this work is necessary.

Just five unknown displacement functions are utilized in the present model against six or more unknown displacement functions used in the other higher-order theories. The most interesting feature of this model is the trigonometric variation of the transverse shear strains in the  $z$ -direction. It satisfies the zero traction on the plate's upper and lowest surfaces without other conditions such as shear correction factors. Analytical solutions of FG plate are obtained, and accuracy is confirmed by comparing the achieved results with those in the literature.

## 2 MATHEMATICAL FORMULATION

### 2.1 KINEMATICS

Based on the present theory and including the transverse normal stress (thickness stretching effect), the kinematic of the plate can be described as

$$(1) \quad \begin{aligned} u(x, y, z, t) &= u_0(x, y, t) - z \frac{\partial w_0}{\partial x} + k_1 f(z) \int \theta(x, y, t) dx, \\ v(x, y, z, t) &= v_0(x, y, t) - z \frac{\partial w_0}{\partial y} + k_2 f(z) \int \theta(x, y, t) dy, \\ w(x, y, z, t) &= w_0(x, y, t) + g(z) \varphi_z(x, y, t), \end{aligned}$$

where

$$(2) \quad k_1 = \alpha^2, \quad k_2 = \beta^2.$$

In this work, the shape function  $f(z)$  is given as follows:

$$(3) \quad f(z) = z \left( \frac{1}{\pi} - \frac{5}{37} \pi \left( \frac{z}{h} \right)^2 \right),$$

where

$$(4) \quad g(z) = \left( \frac{df(z)}{dz} \right).$$

The kinematic relations can be gotten as follows:

$$(5) \quad \begin{aligned} \begin{Bmatrix} \varepsilon_x \\ \varepsilon_y \\ \gamma_{xy} \end{Bmatrix} &= \begin{Bmatrix} \partial u_{0,x} \\ \partial v_{0,y} \\ \partial u_{0,y} + \partial v_{0,x} \end{Bmatrix} - z \begin{Bmatrix} \partial w_{0,xx} \\ \partial w_{0,yy} \\ 2\partial w_{0,xy} \end{Bmatrix} \\ &\quad + f(z) \begin{Bmatrix} k_1 \theta \\ k_2 \theta \\ k_1 \frac{\partial}{\partial y} \int \theta dx + k_2 \frac{\partial}{\partial x} \int \theta dy \end{Bmatrix}, \\ \begin{Bmatrix} \gamma_{yz} \\ \gamma_{xz} \end{Bmatrix} &= g(z) \begin{Bmatrix} k_2 \int \theta dy + \partial \varphi_{z,y} \\ k_1 \int \theta dx + \partial \varphi_{z,x} \end{Bmatrix}, \quad \varepsilon_z = g'(z) \varphi_z. \end{aligned}$$

The integrals terms appeared in the above equations should be resolved by a Navier type method and can be given as follows:

$$(6) \quad \frac{\partial}{\partial y} \int \theta dx = A' \frac{\partial^2 \theta}{\partial x \partial y}, \quad \frac{\partial}{\partial x} \int \theta dy = B' \frac{\partial^2 \theta}{\partial x \partial y}, \quad \int \theta dx = A' \frac{\partial \theta}{\partial x}, \quad \int \theta dy = B' \frac{\partial \theta}{\partial y},$$

where the coefficients  $A'$  and  $B'$  are expressed according to the type of solution used, in this case via Navier.

Therefore,  $A'$ ,  $B'$ ,  $k_1$  and  $k_2$  are expressed as follows:

$$(7) \quad A' = -\frac{1}{\alpha^2}, \quad B' = -\frac{1}{\beta^2}, \quad k_1 = \alpha^2, \quad k_2 = \beta^2,$$

where  $\mu$  and  $\beta$  are used in Eq. 18.

## 2.2 CONSTITUTIVE RELATIONS

The linear constitutive relations of a FG plate can be expressed as

$$(8) \quad \sigma_{ij} = 2\mu\varepsilon_{ij} + \lambda\varepsilon_{kk}\delta_{ij}.$$

The coefficients  $\mu$  and  $\lambda$  in terms of engineering constants are given below:

$$(9) \quad \lambda(z) = \frac{E(z)}{(1-2\nu)(1+\nu)}, \quad \mu(z) = \frac{E(z)}{2(1+\nu)}.$$

## 2.3 EQUATIONS OF MOTION

Hamilton's principle is used herein to derive the equations of motion. The principal can be stated in analytical form as

$$(10) \quad 0 = \int_0^T (\delta U + \delta V - \delta K) dt,$$

where  $\delta U$  is the variation of strain energy;  $\delta V$  is the variation of potential energy;  $\delta K$  is the variation of kinetic energy.

The variation of strain energy of the plate is calculated by

$$(11) \quad \begin{aligned} \delta U &= \int_{-h/2}^{h/2} \int_A [\sigma_x \delta \varepsilon_x + \sigma_y \delta \varepsilon_y + \sigma_z \delta \varepsilon_z + \tau_{xy} \delta \gamma_{xy} + \tau_{yz} \delta \gamma_{yz} + \tau_{xz} \delta \gamma_{xz}] dA dz \\ &= \int_A [N_x \delta \varepsilon_x^0 + N_y \delta \varepsilon_y^0 + N_z \delta \varepsilon_z^0 + N_{xy} \delta \gamma_{xy}^0 + M_x^b \delta k_x^b + M_y^b \delta k_y^b \\ &\quad + M_{xy}^b \delta k_{xy}^b + M_x^s \delta k_x^s + M_y^s \delta k_y^s + M_{xy}^s \delta k_{xy}^s + S_{yz}^S \delta \gamma_{yz} + S_{xz}^S \delta \gamma_{xz}] dA = 0, \end{aligned}$$

where  $A$  is the surface. Substituting Eqs. (5) into Eqs. (11), the resulting forces and moments  $N$ ,  $M$  and  $S$  can be obtained by simply integrating stress as given in the second expression of strain energy.

The variation of potential energy of the applied loads can be expressed as

$$(12) \quad \delta V = - \int_A q \delta(w_0(x, y, t) + g(z)\varphi_z(x, y, t)) dA,$$

where  $q$  is the distributed transverse load.

The variation of kinetic energy of the plate can be written as

$$(13) \quad \begin{aligned} \delta K &= \int_{-h/2}^{h/2} \int_A [\dot{u}\delta\dot{u} + \dot{v}\delta\dot{v} + \dot{w}\delta\dot{w}] \rho(z) dA dz \\ &= \int_A \left\{ I_0[\dot{u}_0\delta\dot{u}_0 + \dot{v}_0\delta\dot{v}_0 + \dot{w}_0\delta\dot{w}_0] \right. \\ &\quad - I_1[\dot{u}_0\delta\dot{w}_{0,x} + \dot{v}_0\delta\dot{w}_{0,y} + \dot{w}_{0,x}\delta\dot{u}_0 + \dot{w}_{0,y}\delta\dot{v}_0] \\ &\quad + I_2[\dot{w}_{0,x}\delta\dot{w}_{0,x} + \dot{w}_{0,y}\delta\dot{w}_{0,y}] \\ &\quad - J_1[\dot{u}_0\delta\dot{\theta}_{,x} + \dot{\theta}_{,x}\delta\dot{u}_0 + \dot{v}_0\delta\dot{\theta}_{,y} + \dot{\theta}_{,y}\delta\dot{v}_0] \\ &\quad + J_2[\dot{w}_{0,x}\delta\dot{\theta}_{,x} + \dot{\theta}_{,x}\delta\dot{w}_{0,x} + \dot{w}_{0,y}\delta\dot{\theta}_{,y} + \dot{\theta}_{,y}\delta\dot{w}_{0,y}] \\ &\quad \left. + K_2[\dot{\theta}_{,x}\delta\dot{\theta}_{,x} + \dot{\theta}_{,y}\delta\dot{\theta}_{,y}] + J_1^s[\dot{w}_0\delta\dot{\varphi}_z + \dot{\varphi}_z\delta\dot{w}_0] + K_2^s\dot{\varphi}_z\delta\dot{\varphi}_z \right\} dA, \end{aligned}$$

where dot-superscript convention indicates the differentiation with respect to the time variable  $t$ ; and  $I_0, I_1, J_1, I_2, J_2, K_2, K_2^s$  are mass inertias defined as

$$(14) \quad (I_0, I_1, J_1, J_1^s, I_2, J_2, K_2, K_2^s) = \int_{-h/2}^{h/2} (1, z, f, g, z^2, zf, f^2, g^2) \rho(z) dz.$$

Substituting the expressions of  $\delta U$ ,  $\delta V$  and  $\delta K$  from Eqs. (11), (12), and (13) into Eq. (10) integrating by parts, and assembling the coefficients of  $\delta u_0$ ,  $\delta v_0$ ,  $\delta w_0$ ,  $\delta\theta$ , and  $\delta f_z$ , the following corresponding equations of the plate are obtained:

$$(15a) \quad \delta u_0 : \frac{\partial N_x}{\partial x} + \frac{\partial N_{xy}}{\partial y} = I_0 \ddot{u}_0 - I_1 \frac{\partial \ddot{w}_0}{\partial x} - J_1 \frac{\partial \ddot{\theta}}{\partial x},$$

$$(15b) \quad \delta v_0 : \frac{\partial N_{xy}}{\partial x} + \frac{\partial N_y}{\partial y} = I_0 \ddot{v}_0 - I_1 \frac{\partial \ddot{w}_0}{\partial y} - J_1 \frac{\partial \ddot{\theta}}{\partial y},$$

$$(15c) \quad \begin{aligned} \delta w_0 : \frac{\partial^2 M_x^b}{\partial x^2} + 2 \frac{\partial^2 M_{xy}^b}{\partial x \partial y} + \frac{\partial^2 M_y^b}{\partial y^2} + q \\ = I_0(\ddot{w}_0 + \ddot{\theta}) + I_1 \left( \frac{\partial \ddot{u}_0}{\partial x} + \frac{\partial \ddot{v}_0}{\partial y} \right) - I_2 \nabla^2 \ddot{w}_0 - J_2 \ddot{\theta} + J_1^s \ddot{\varphi} \end{aligned}$$

$$\begin{aligned}
(15d) \quad \delta\theta : & -k_1 M_x^s - k_2 M_y^s - (k_1 A' + k_2 B') \frac{\partial^2 M_{xy}^s}{\partial x \partial y} \\
& + k_1 A' \frac{\partial S_{xz}^s}{\partial x} + k_2 B' \frac{\partial S_{yz}^s}{\partial y} + q \\
& = I_0(\ddot{w}_0 + \ddot{\theta}) + J_1 \left( \frac{\partial \ddot{u}_0}{\partial x} + \frac{\partial \ddot{v}_0}{\partial y} \right) - J_2 \nabla^2 \ddot{w}_0 - K_2 \ddot{\theta} + J_1^s \ddot{\varphi},
\end{aligned}$$

$$(15e) \quad \delta\varphi_z : \frac{\partial S_{xz}^s}{\partial x} + \frac{\partial S_{yz}^s}{\partial y} - N_z = J_1^s(\ddot{w}_0 + \ddot{\theta}) + K_2^s \ddot{\varphi}.$$

### 3 EXACT SOLUTION FOR SIMPLY SUPPORTED FG PLATE

Rectangular plates are generally classified according to the type of support used. This paper is concerned with the exact solutions of Eqs. (15a)–(15e) for a simply supported FG plate.

The following boundary conditions are imposed at the edges:

$$\begin{aligned}
(16) \quad v_0 = w_0 = \theta = \frac{\partial \theta}{\partial y} = \varphi = N_x = M_x^b = M_x^s = 0 \quad \text{at } x = 0, a \\
u_0 = w_0 = \theta = \frac{\partial \theta}{\partial x} = \varphi = N_y = M_y^b = M_y^s = 0 \quad \text{at } y = 0, b
\end{aligned}$$

Following the Navier solution procedure, the authors assume the following solution from for  $u_0$ ,  $v_0$ ,  $w_0$ ,  $\theta$  and  $f_z$  that satisfies the boundary conditions given in Eq. (16):

$$(17) \quad \begin{Bmatrix} u_0 \\ v_0 \\ w_0 \\ \theta \\ \varphi^z \end{Bmatrix} = \sum_{m=1}^{\infty} \sum_{n=1}^{\infty} \begin{Bmatrix} U_{mn} e^{i\omega t} \cos(\lambda x) \sin(\mu y) \\ V_{mn} e^{i\omega t} \sin(\lambda x) \cos(\mu y) \\ W_{mn} e^{i\omega t} \sin(\lambda x) \sin(\mu y) \\ X_{mn} e^{i\omega t} \sin(\lambda x) \sin(\mu y) \\ \Phi_{mn} e^{i\omega t} \sin(\lambda x) \sin(\mu y) \end{Bmatrix},$$

where  $U_{mn}$ ,  $V_{mn}$ ,  $W_{mn}$ ,  $X_{mn}$  and  $\Phi_{mn}$  are arbitrary parameters,  $\omega$  is the natural fundamental frequency; and  $\lambda$ ,  $\mu$  are defined as

$$(18) \quad \mu = m\pi/a \quad \text{and} \quad \beta = n\pi/b.$$

Substituting Eq. (17) and (18) into Eqs. (15a)–(15e), the analytical solutions can be obtained from

$$\begin{aligned}
(19) \quad ([a_{ij}] - \omega^2 [m_{ij}]) \{ U_{mn} \quad V_{mn} \quad W_{mn} \quad X_{mn} \quad \Phi_{mn} \}^T \\
= \{ 0 \quad 0 \quad 0 \quad 0 \quad 0 \}^T, \quad i = j = 1, \dots, 5,
\end{aligned}$$

in witch

$$\begin{aligned}
(20) \quad a_{11} &= -(A_{11}\alpha^2 + A_{66}\beta^2), & a_{12} &= -\alpha\beta(A_{12} + A_{66}), \\
a_{13} &= \alpha(B_{11}\alpha^2 + (B_{12} + 2B_{66})\beta^2), \\
a_{14} &= -\alpha(B_{11}^s A'k_1\alpha^2 + B_{12}^s B'k_2\beta^2 + B_{66}^s(A'k_1 + B'k_2)\beta^2), \\
a_{15} &= L\alpha, & a_{22} &= -\alpha^2 A_{66} - \beta^2 A_{22}, \\
a_{23} &= \beta(B_{22}\beta^2 + (B_{12} + 2B_{66})\alpha^2), \\
a_{24} &= -\beta[B_{22}^s B'k_2\beta^2 + \alpha^2(B_{12}^s A'k_1 + B_{66}^s(A'k_1 + B'k_2))], \\
a_{25} &= L\beta, & a_{33} &= -\alpha^2(D_{11}\alpha^2 + (2D_{12} + 4D_{66})\beta^2) - D_{22}\beta^4, \\
a_{34} &= D_{11}^s A'k_1\alpha^4 + D_{12}^s(A'k_1 + B'k_2)\beta^2\alpha^2 + D_{22}^s B'k_2\beta^4 \\
&\quad + 2D_{66}^s(A'k_1 + B'k_2)\beta^2\alpha^2, \\
a_{35} &= -L^a(\alpha^2 + \beta^2), \\
a_{44} &= -(2(k_1\beta^2 H_{66}^s + H_{66}^s\alpha^2 k_2) + k_1(H_{11}^s\alpha^2 + \beta^2 H_{12}^s + A_s^{44}) \\
&\quad + k_2(\beta^2 H_{22}^s + A_s^{55} + H_{12}^s\alpha^2)) \\
a_{45} &= -[A_{44}^s\alpha^2 + A_{55}^s\beta^2 + R(\alpha^2 + \beta^2)], \\
a_{55} &= -(A_{44}^s\alpha^2 + A_{55}^s\beta^2 + R^a)
\end{aligned}$$

and

$$\begin{aligned}
(21) \quad m_{11} &= m_{22} = -I_0, & m_{13} &= \alpha I_1, & m_{14} &= \alpha J_1, & m_{23} &= \beta I_1, \\
m_{24} &= \beta J_1, & m_{33} &= -[I_0 + I_2(\alpha^2 + \beta^2)], & m_{34} &= -[I_0 + J_2(\alpha^2 + \beta^2)], \\
m_{44} &= -[I_0 + K_2(\alpha^2 + \beta^2)], & m_{35} &= m_{45} = -J_1^s, & m_{55} &= -K_2^s;
\end{aligned}$$

non-dimensional parameters:

$$(22) \quad \hat{\omega} = \omega h \sqrt{\frac{\rho}{G}}, \quad \tilde{\omega} = \omega \frac{a^2}{\pi^2} \sqrt{\frac{\rho h}{D}}, \quad D = \frac{Eh^3}{12(1-\nu^2)}, \quad \bar{\omega} = \omega h \sqrt{\frac{\rho_m}{E_m}}.$$

#### 4 NUMERICAL RESULTS

In this section, various numerical examples are presented for free vibration analyses of a simply supported FG plate. The proposed model will be first validated through the comparison with the existing data available in literature. For this, two types of FGMs plates are considered: Al/Al<sub>2</sub>O<sub>3</sub> and Al/ZrO<sub>2</sub>.

The material properties of FG plates are reported in Table 1.

For validation of the present improved theory, as a first example (Table 2). a comparison parameters of non-dimensional natural frequency is realized for an isotropic

Table 1: Material proprieties used in the FG plates

Proprieties	Metal		Ceramic		
	Al	A*	A <sub>2</sub> O <sub>3</sub>	ZrO <sub>2</sub>	ZrO <sub>2</sub> *
E (Gpa)	70	68.9	380	200	211
$\nu$	0.3	0.33	0.3	0.3	0.33
$P$ (kg/m <sup>3</sup> )	2702	2700	3800	5700	4500

rectangular plate, with the solution of Srinivas et al. [30] based on three-dimensional elasticity solutions, Reddy and Phan [31] based on third-order shear deformation theory, Abualnour et al. [29] and Hebali et al. [27] founded on quasi-3D shear deformation theory. The results of the present theory approve very well with the 3D and quasi-3D theories. However, the third shear deformation plate theory [31], which neglected the stretching effect ( $\varepsilon_z = 0$ ), slightly underestimates frequency in comparison to the present quasi-3D theory and 3D.

Table 2: Non-dimensional natural frequencies  $\hat{\omega}$  of Al/Al<sub>2</sub>O<sub>3</sub> an isotropic plate with  $\nu = 0.3$ ,  $a/h = 10$  and  $a/b = 1$ 

$m$	$n$	Present $\varepsilon_z \neq 0$	Hebali et al. [27] $\varepsilon_z \neq 0$	Abualnour et al. [29] $\varepsilon_z \neq 0$	Srinivas et al. [30] 3-D	Reddy and Phan [31]
1	1	<b>0.0933</b>	0.0933	0.0933	0.0932	0.0931
1	2	<b>0.2230</b>	0.2228	0.2231	0.2226	0.2222
2	2	<b>0.3424</b>	0.3422	0.3429	0.3421	0.3411
1	3	<b>0.4175</b>	0.4173	0.4182	0.4171	0.4158
2	3	<b>0.5241</b>	0.5240	0.5254	0.5239	0.5221
3	3	<b>0.6892</b>	0.6890	0.6912	0.6889	0.6862
2	4	<b>0.7514</b>	0.7512	0.7537	0.7511	0.7481
1	5	<b>0.9268</b>	0.9268	0.9305	0.9268	0.9230
4	4	<b>1.0890</b>	1.0890	1.0938	1.0889	1.0847

In the next example (Table 3), the validation of the obtained results is carried out for the present quasi-3D model by comparing with those computed via the 3D Ritz method presented by Liew et al. [32], 3D elasticity solutions presented by Alibeigloo [33] and Quasi-3D trigonometric plate theory presented by Bessaim et al. [34]. It can be observed that the results of the 3D Ritz method presented by Liew et al. [32] and 3D elasticity solutions presented by Alibeigloo [33] are to bring nearer to the present results. Also, Table 3 reveals that the current theory only gives appropriate results to those achieved by the quasi-3D plate theory developed by Bessaim et al. [34]. This demonstrates that identical precision is achievable with the suggested model.



Table 3: Comparison of dimensionless first dimensionless natural frequency  $\bar{\omega}$  of Al/Al<sub>2</sub>O<sub>3</sub> the isotropic rectangular plate ( $a/b = 1.5$ )

Theory	$a/h$				
	5/2	10/3	5	10	100
Abualnour et al. [29], $\varepsilon_z \neq 0$	1.0996	1.2122	1.3237	1.4120	1.446
3D Ritz method, Liew et al. [32]	1.0954	1.2088	1.3209	1.4096	1.444
Elasticity 3D, r Alibeigloo [33]	1.0940	1.2075	1.3200	1.4096	1.444
Bessaim et al. [34] $\varepsilon_z \neq 0$	1.0996	1.2122	1.3237	1.4120	1.446
Present $\varepsilon_z \neq 0$	<b>1.0959</b>	<b>1.2098</b>	<b>1.3229</b>	<b>1.4125</b>	<b>1.447</b>

The non-dimensional fundamental frequency variation  $\bar{\omega}$  is illustrated in Fig. 1 of simply supported edges FG plate rectangular plates versus the material index  $k$  for three values of the side-to-thickness ratios ( $a/h$ ). Whereas a rapid increase of the non-dimensional fundamental natural frequency until a value of  $k = 2$ . Proceeding from this value, the natural frequency end to keep a more or less constant shape. On the other hand, the increase in the  $a/h$  ratio tends to decrease frequencies. In other words, the frequencies decrease as the thickness of the plate increases.

Figure 2 presents the fundamental natural frequency variation of  $\bar{\omega}$  of simply supported edges FG plate versus the geometrical ratio ( $b/a$ ) for different values of the side-to-thickness ratios ( $a/h$ ). The highest frequencies are obtained for a square plate ( $b/a = 1$ ).

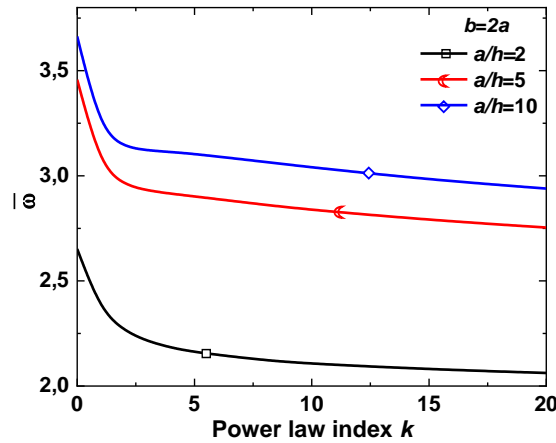


Fig. 1: Non-dimensional fundamental frequency  $\bar{\omega}$  of FG rectangular plates with simply supported edges ( $b = 2a$ ) as a function of material gradient index ( $k$ ) for different  $a/h$ .

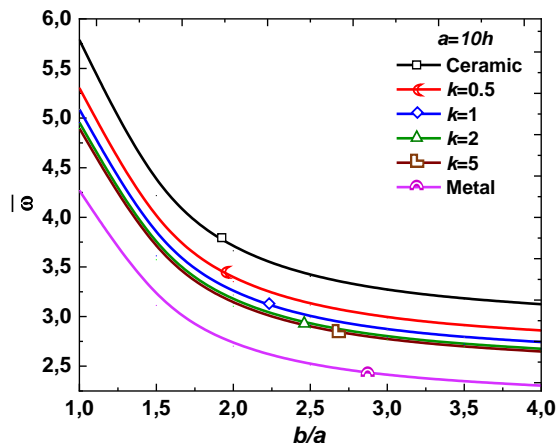


Fig. 2: Non-dimensional fundamental frequency  $\bar{\omega}$  of simple supported FG plates as a function of aspect ratio ( $b/a$ ) for different material gradient index ( $k$ ) for  $a/h = 10$ .

Figure 3 illustrates the variation of the non-dimensional fundamental natural frequency  $\bar{\omega}$  of simply supported FG plate rectangular plates as a function of the side-to-thickness ratio ( $a/h$ ). As observed, the evolution in the ( $a/h$ ) ratio increases the frequencies, and the increase in the material index  $k$  reduces them. Also, the homogeneous ceramic plate has the highest frequency.

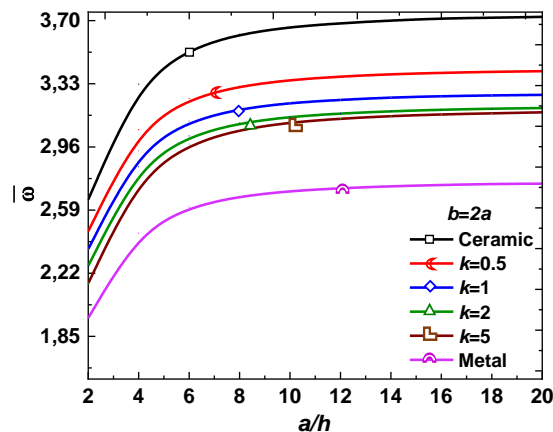


Fig. 3: Non-dimensional fundamental frequency  $\bar{\omega}$  of simply supported FG rectangular plates ( $b = 2a$ ) as a function of side to thickness ratio ( $a/h$ ) for different material index ( $k$ ).

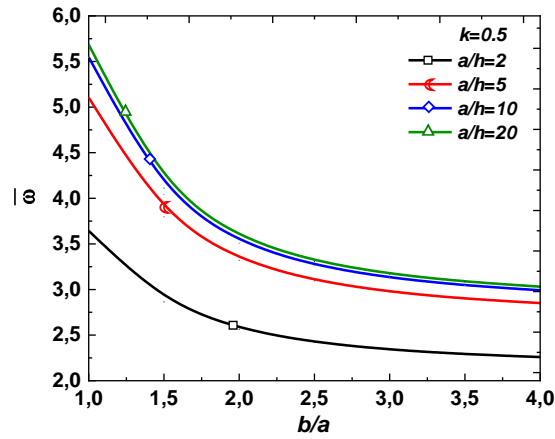


Fig. 4: Non-dimensional fundamental frequency  $\bar{\omega}$  of simply supported FG plates as a function of aspect ratio ( $b/a$ ) for different side to thickness ratio ( $a/h$ ) with  $k = 0.2$ .

In Fig.4, we have plotted the same variation but for different values of the material index  $k$ . The highest frequencies are achieved for a homogeneous ceramic plate and the lowest for a metal plate. The increase in index  $k$  decreases the frequencies.

The variation of the non-dimensional fundamental natural frequency  $\bar{\omega}$  of simply supported FG plate is given in Fig. 5 for the various values of  $E_m/E_c$ . It is clear that the increase in ratio  $E_m/E_c$  increases the frequencies, and the increase in the power index  $k$  reduces them.

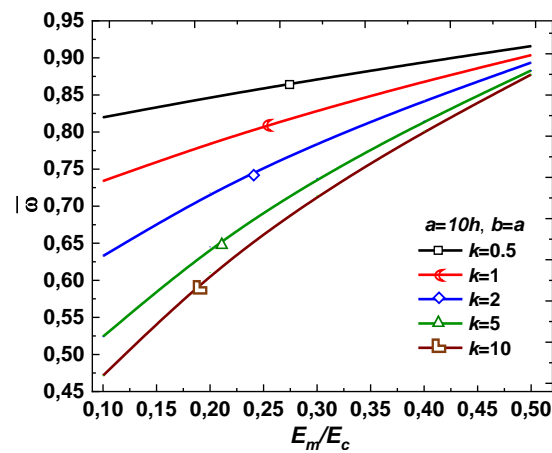


Fig. 5: Non-dimensional fundamental frequency  $\bar{\omega}$  of simply supported FG plates as a function of anisotropy ratio  $E_m/E_c$  ( $a/h = 10, b/a = 1$ ).

## 5 CONCLUSIONS

Free vibration analyses of FG plates are realized using an improved quasi-3D theory, including the stretching effects. This theory considers hyperbolic function shape to describe the variation of transverse shear stress and respects the nullity conditions on the top and bottom surfaces of the plate. The kinematic of the current model is adjusted by considering integral terms, which results in a reduced number of unknowns compared with other theories. Various examples show that the current theory is more accurate than other HSDTs, which use variables. Based on the present work, some of the highlighted conclusions are summarized as follows:

- The accuracy of the current theory has been checked, and an excellent agreement is observed.
- The inclusion of the stretching effect ( $\varepsilon_z \neq 0$ ) leads to an increase in the fundamental natural frequency.
- The quasi-3D model has a significant role for thick and moderately thick FG plates and must be considered in the modeling and calculation process.
- The present quasi-3D theory is accurate and straightforward in forecasting the vibration analysis of FG plates.

## REFERENCES

- [1] M. Koizumi (1997). FGM activities in Japan. *Composites Part B: Engineering* **28**(1-2) 1-4.
- [2] Wang Baochen (2005) Electromagnetic centrifugal casting of ceramic particle reinforced aluminum matrix composites [D].
- [3] Y. Li (2000) Research and application of functionally graded materials [J]. *Metallic Functional Materials* **7**(4) 15-23 (in Chinese).
- [4] R. Huang (2016) Optimization design and research progress of functionally graded thermoelectric materials [J]. *Journal of Chifeng University (NATURAL SCIENCE EDITION)* **32**(24) 33-34.
- [5] G. Bao, L. Wang (1995) Multiple cracking in functionally graded ceramic/metal coatings. *International Journal of Solids and Structures* **32** 2853-2871.
- [6] P.R. Marur (1999) "Fracture Behaviour of Functionally Graded Materials". PhD Thesis, Auburn University, Alabama.
- [7] Naotake Noda (1999) Thermal stresses in functionally graded materials. *Journal of Thermal Stresses* **22** 477-512.
- [8] M.D. Demirbaş, M.K. Apalak (2018) Thermal Residual Stresses Analyses of Two-Dimensional Functionally Graded Circular Plates with Temperature-Dependent Material Properties. *International Journal of Engineering Research and Development* **10**(2) 203-213.

- [9] O. Kesler, M. Finot, S. Sampath (1997) Determination of processing-induced stresses and properties of layered and graded coatings: experimental method and results for plasma-sprayed NiAl<sub>2</sub>O<sub>3</sub>. *Acta Materialia* **45** 3123-3134.
- [10] G. Kirchhoff (1876) "Vorlesungen über mathematische Physik", Vol. 1. B.G. Teubner, Leipzig.
- [11] A.E.H. Love (1926) "A Treatise on the Mathematical Theory of Elasticity", 4th ed. Cambridge University Press, Cambridge, 1926.
- [12] E. Reissner (1954) The Effect of Transverse Shear Deformation on the Bending of Elastic Plates. *Journal of Applied Mechanics* **12** A69-A77.
- [13] R.D. Mindlin (1951) Influence of Rotatory Inertia and Shear on Flexural Motions of Isotropic Elastic Plates. *Journal of Applied Mechanics* **18** 31-38.
- [14] A.M. Zenkour (2006) Generalized shear deformation theory for bending analysis of functionally graded plates. *Applied Mathematical Modelling* **30** 67-84.
- [15] M. Bodaghi, A.R. Saidi (2010) Levy-type solution for buckling analysis of thick functionally graded rectangular plates based on the higher-order shear deformation plate theory. *Applied Mathematical Modelling* **34**(11) 3659-3673.
- [16] A. Benachour, H.D. Tahara, H.A. Atmanea, A. Tounsi, M.S. Ahmed (2011) A four variable refined plate theory for free vibrations of functionally graded plates with arbitrary gradient. *Composites Part B: Engineering* **42**(6) 1386-1394.
- [17] H.T. Thai, S.E. Kim (2013) A simple higher-order shear deformation theory for bending and free vibration analysis of functionally graded plates. *Composite Structures* **96** 165-173.
- [18] L.V. Tran, A.J.M. Ferreira, H. Nguyen-Xuan (2013) Isogeometric analysis of functionally graded plates using higher-order shear deformation theory. *Composites Part B: Engineering* **51** 368-383.
- [19] J.L. Mantari, C.G. Soares (2014) Static response of advanced composite plates by a new non-polynomial higher-order shear deformation theory. *International Journal of Mechanical Sciences* **78** 60-71.
- [20] B. Merazka, A. Bouhadra, A. Menasria, M.M Selim, A.A. Bousahla, F. Bourada, A. Tounsi, K.H. Benrahou, A. Tounsi, M.M. Al-Zahrani (2021) Hygro-thermo-mechanical bending response of FG plates resting on elastic foundations. *Steel and Composite Structures* **39**(5) 631-643.
- [21] B. Rebai, A. Bouhadra, A.A. Bousahla, M. Meradjah, F. Bourada, A. Tounsi, A. Tounsi, M. Hussain (2021) and M.: Thermoelastic response of functionally graded sandwich plates using a simple integral HSDT. *Archive of Applied Mechanics* **91** 3403-3420.
- [22] A.M. Zenkour (2007) Benchmark trigonometric and 3-d elasticity solutions for an exponentially graded thick rectangular plate. *Archive of Applied Mechanics* **77**(4) 197-214.
- [23] H. Matsunaga (2008). Free vibration and stability of functionally graded plates according to a 2-D higher-order deformation theory. *Composite Structures* **82** 499-512.
- [24] A.M. Neves, A.J.M. Ferreira, E. Carrera, C.M.C. Roque, M. Cinefra, R.M.N. Jorge, et al. (2012) A quasi-3D sinusoidal shear deformation theory for the static and free

- vibration analysis of functionally graded plates. *Composites Part B: Engineering* **43** 711-25.
- [25] D.K. Jha, T. Kant, R.K. Singh (2013) Free vibration response of functionally graded thick plates with shear and normal deformations effects. *Composite Structures* **96** 799-823.
- [26] S.A. Sheikholeslami, A.R. Saidi (2013) Vibration analysis of functionally graded rectangular plates resting on elastic foundation using higher-order shear and normal deformable plate theory. *Composite Structures* **106** 350-61.
- [27] H. Hebali, A. Tounsi, M.S.A. Houari, A. Bessaim, E.A. Adda Bedia (2014) New Quasi-3D Hyperbolic Shear Deformation Theory for the Static and Free Vibration Analysis of Functionally Graded Plates. *Journal of Engineering Mechanics* **140**(2) 374-383.
- [28] F. Alijani, M. Amabili (2014) Effect of thickness deformation on large-amplitude vibrations of functionally graded rectangular plates. *Composite Structures* **113** 89-107.
- [29] M. Abualnour, M.S.A. Houari, A. Tounsi, E.A. Adda Bedia, S.R. Mahmoud (2017) A novel quasi-3D trigonometric plate theory for free vibration analysis of advanced composite plates. *Composite Structures* **184** 688-697.
- [30] S. Srinivas, C.V. Joga, A.K. Rao (1970) An exact analysis for vibration of simply supported homogeneous and laminated thick rectangular plates. *Journal of Sound and Vibration* **12**(2) 187-199.
- [31] J.N. Reddy, N.D. Phan (1985) Stability and vibration of isotropic, orthotropic and laminated plates according to a higher-order shear deformation theory. *Journal of Sound and Vibration* **98**(2) 157-170.
- [32] K.M. Liew, K.C. Hung, M.K. Lim (1993). A continuum three-dimensional vibration analysis of thick rectangular plates. *International Journal of Solids and Structures* **30**(24) 3357-3379.
- [33] A. Alibeigloo (2011). Free vibration analysis of nano-plate using three-dimensional theory of elasticity. *Acta Mechanica* **222**(1) 149-159.
- [34] A. Bessaim, M.S.A. Houari, F. Bernard, A. Tounsi (2015) A nonlocal quasi-3D trigonometric plate model for free vibration behaviour of micro/nanoscale plates. *Structural Engineering and Mechanics* **56**(2) 223-240.